Protein Science (1993), 2, 1291–1300. Cambridge University Press. Printed in the USA.

Effect of pH and denaturants on the folding and stability of murine interleukin-6

LARRY D. WARD,[1] JIAN GUO ZHANG,[1] GREG CHECKLEY,[2]
BARRY PRESTON,[2] AND RICHARD J. SIMPSON[1]

[1] Joint Protein Structure Laboratory, Ludwig Institute for Cancer Research and
The Walter and Eliza Hall Institute for Medical Research, Parkville, Victoria 3050, Australia
[2] Department of Biochemistry, Monash University, Clayton, Victoria 3168, Australia

(RECEIVED February 9, 1993; REVISED MANUSCRIPT RECEIVED April 30, 1993)

Abstract

The conformation and stability of a recombinant mouse interleukin-6 (mIL-6) has been investigated by analytical ultracentrifugation, fluorescence spectroscopy, urea-gradient gel electrophoresis, and near- and far-ultraviolet circular dichroism. On decreasing the pH from 8.0 to 4.0, the tryptophan fluorescence of mIL-6 was quenched 40%, the midpoint of the transition occurring at pH 6.9. The change in fluorescence quantum yield was not due to unfolding of the molecule because the conformation of mIL-6, as judged by both urea-gradient gel electrophoresis and CD spectroscopy, was stable over the pH range 2.0–10.0. Sedimentation equilibrium experiments indicated that mIL-6 was monomeric, with a molecular mass of 22,500 Da over the pH range used in these physicochemical studies. Quenching of tryptophan fluorescence (20%) also occurred in the presence of 6 M guanidine hydrochloride upon going from pH 7.4 to 4.0 suggesting that an amino acid residue vicinal in the primary structure to one or both of the two tryptophan residues, Trp-36 and Trp-160, may be partially involved in the quenching of endogenous fluorescence. In this regard, similar results were obtained for a 17-residue synthetic peptide, peptide H1, which corresponds to an N-terminal region of mIL-6 (residues Val-27–Lys-43). The pH-dependent acid quenching of endogenous tryptophan fluorescence of peptide H1 was 30% in the random coil conformation and 60% in the presence of α-helix-promoting solvents. Replacement of His-33 with Ala-33 in peptide H1 alleviated a significant portion of the pH-dependent quenching of fluorescence suggesting that the interaction of the imidazole ring of His-33 with the indole ring of Trp-36 is a major determinant responsible for the quenching of the endogenous protein fluorescence of mIL-6.

Keywords: circular dichroism; denaturation; fluorescence studies; interleukin-6; protein structure

Interleukin-6 is a multifunctional cytokine that acts on a wide variety of tissues to elicit a broad spectrum of biological functions including terminal differentiation of B cells, growth and differentiation of T cells, and regulation of the acute-phase responses. IL-6 is also capable of inducing the differentiation of hematopoietic progenitor cells and megakaryocytes (for reviews see Kishimoto [1989], Van Snick [1990], and Gordon & Hoffman [1992]). Furthermore, IL-6 has been reported to be causally associated with multiple myeloma (Klein & Bataille, 1991) as well as several autoimmune diseases (Hirano et al., 1990).

Mouse IL-6, a 187-residue glycoprotein, has been sequenced at both the protein (Simpson et al., 1988a) and DNA level (Van Snick et al., 1988). It contains four cysteine residues and one O-glycosylation site (Simpson et al., 1988a). In an earlier report we described the synthesis of mIL-6 as a fusion protein using a *lac* operon-inducible plasmid in *Escherichia coli*, the first eight amino acids being from the N-terminus of bacterial β-galactosidase and the last 176 amino acids corresponding to residues 12–187 of native mIL-6 (Simpson et al., 1988b). To obtain sufficient quantities of material for biophysical studies, we developed a large-scale procedure for rapidly extracting and purifying recombinant mIL-6 from "inclusion bodies" (Zhang et al., 1992). Biological and chemical char-

Reprint requests to: Richard J. Simpson, Ludwig Institute for Cancer Research, P.O. Royal Melbourne Hospital, Parkville, Victoria 3050, Australia.

Abbreviations: IL-6, interleukin-6; m-, murine; h-, human; GdnHCl, guanidine hydrochloride; SDS, sodium dodecyl sulfate; MES, 2-(*N*-morpholino)ethane sulfonic acid; S, weight average sedimentation coefficient; $[\theta]_{MRW}$, mean residue ellipticity; HEPES, *N*-2-hydroxyethylpiperazine-N^1-2-ethane sulfonic acid; Tris, Tris(hydroxymethyl)aminomethane; CAPS, 3-(cyclohexylamino)-1-propane sulfonic acid; TFE, trifluoroethanol; GM-CSF, granulocyte-macrophage colony-stimulating factor.

acterization of the *E. coli*-derived mIL-6, including the positions of the two intramolecular disulfide bonds, have been reported previously (Simpson et al., 1988b; Zhang et al., 1992).

We are currently using site-directed mutagenesis to probe the structure–function relationships of mIL-6. The interpretation of such mutation experiments is often only clear when the folding and conformational state of the mutant can be understood in detail. If the activity of a mutant protein is unaffected by the mutation then the residue is unlikely to have a critical role in the folding or activity of the protein. However, if the mutation results in a partial or complete loss of activity then it is important to establish whether this is a consequence of incorrect folding, instability, aggregation, or the disruption of its receptor interaction motif. In the present study we have determined the conformational and stability characteristics of purified "wild-type" recombinant mIL-6.

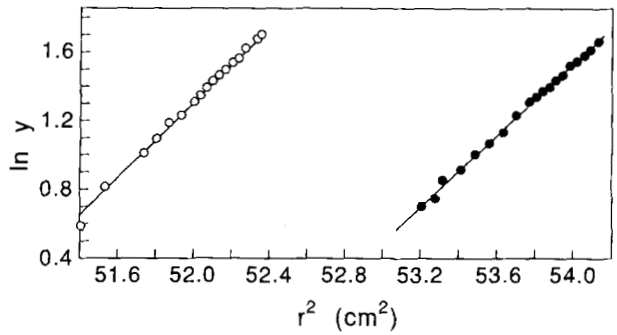

Fig. 1. Dependence of molecular weight of recombinant mIL-6 on pH. Sedimentation equilibrium analytical centrifugation of recombinant mIL-6 equilibrated in 10 mM HEPES, pH 7.4 (●), and in 10 mM sodium acetate, pH 4.0 (○). Data are plotted as ln y vs. r^2, where y is the relative concentration of protein calculated as fringes, and r^2 is the square of the distance from the axis of rotation. The indicated lines were evaluated from a least-squares fit of the data.

Results

Molecular mass

The hydrodynamic properties of mIL-6 were investigated by sedimentation velocity analysis using a protein concentration of 2 mg/mL in 10 mM sodium acetate buffer, pH 4.0. Under these conditions mIL-6 migrated as a symmetrical peak as expected for a homogeneous protein. The sedimentation of mIL-6 was described by a coefficient of 2.74S. A similar analysis carried out at pH 7.4 (10 mM HEPES buffer) yielded a sedimentation value of 2.53S (data not shown). The results indicate that the hydrodynamic volume of mIL-6 is not sensitive to a variation of buffer composition or pH.

mIL-6 did exhibit a tendency to aggregate upon increasing the ionic strength of the buffer. When mIL-6 (2 mg/mL) was subjected to sedimentation velocity analysis in 10 mM sodium acetate buffer, pH 4.0 containing 0.15 M NaCl, large aggregates were observed to sediment to the bottom of the cell (data not shown).

The concentration and pH dependence of the molecular weight of mIL-6 in low ionic strength buffer was investigated further by sedimentation equilibrium analysis using the meniscus-depletion method of Yphantis (1964). Data were analyzed in terms of Rayleigh interferograms. The plots of ln y vs. r^2, where y is the relative concentration of mIL-6 expressed in terms of Rayleigh fringes and r^2 is the square of the distance from the center of the axis of rotation, are given in Figure 1 for mIL-6 in 10 mM sodium acetate buffer, pH 4.0. The linear plot observed was consistent with a homogeneous protein solution and indicated that no concentration-dependent self association was occurring over the concentration range spanned in the experiment (0.1–0.3 mg/mL). Utilizing a slope value of 0.986 ± 0.009 and a partial specific volume of 0.737, calculated on the basis of the amino acid composition (Cohn & Edsall, 1943), a molecular mass of 19,800 ± 200 Da was determined. Sedimentation equilibrium analysis of mIL-6 was also performed at pH 7.4 using 10 mM HEPES buffer (Fig. 1). Again a linear dependence of ln y vs. r^2 was observed. The data were best fit by a line of slope of 1.123 ± 0.015, which leads to a weight average molecular mass of 22,500 ± 300 Da. This finding was similar to that obtained at pH 4.0 and indicated that the change in pH was not inducing a change in the polymerization state of mIL-6.

Dependence of the conformational properties of mIL-6 on pH

Fluorescence measurements

An excitation wavelength of 295 nm was utilized in order to preferentially excite the two tryptophan residues of mIL-6 (Trp-36 and Trp-160). The fluorescence emission spectrum of mIL-6 was sensitive to pH (Fig. 2A). Upon increasing the pH from 2.0 to 8.0 the relative fluorescence of mIL-6 increased 1.7-fold with a transition midpoint occurring at pH 6.9 (Fig. 2B). This transition was readily reversible. Dilution of mIL-6 from sodium acetate buffer (pH 4.0) into HEPES buffer (pH 7.4) alleviated the quenching of the tryptophan residues observed at the lower pH. The pH-induced change in quantum yield of the tryptophan residues was accompanied by a small blue shift in the emission maximum from 348 nm at pH 8.5 to 345 nm at pH 4.0 (Fig. 2A). The fluorescence properties of *N*-acetyltryptophanamide were essentially constant over the same pH range (Fig. 2B), which indicated that the acid-induced change in intensity of mIL-6 fluorescence is a specific effect and results from either a change in conformation or a localized interaction between the tryptophan side chain and an ionizable residue.

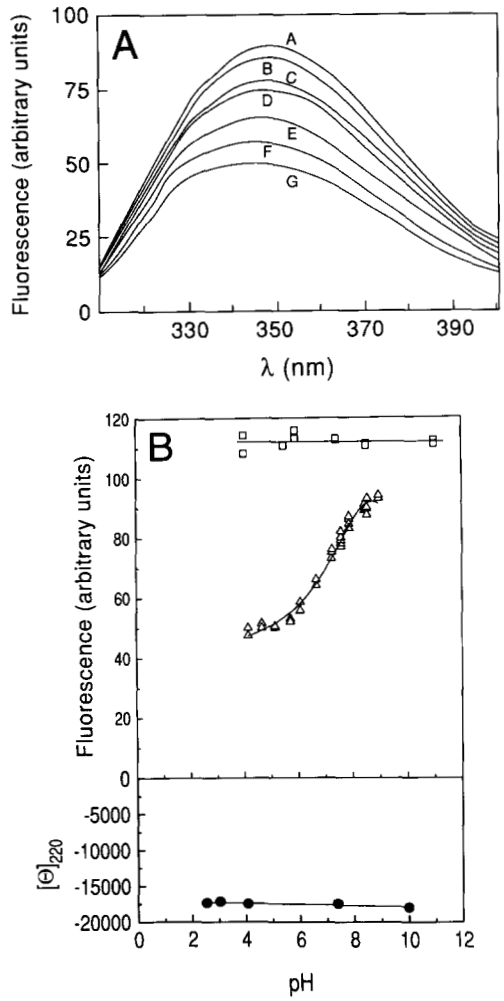

Fig. 2. Dependence of the intrinsic protein fluorescence and CD signal of recombinant mIL-6 on pH. **A:** Fluorescence emission spectra as a function of pH. Spectra A–G correspond to pH values of 8.5, 7.9, 7.5, 7.2, 6.7, 6.0, and 4.1, respectively. All spectra and single wavelength readings were recorded at 25 °C using a 295-nm excitation wavelength and 5-nm excitation and emission slits. Protein concentration of mIL-6 was 30 μg/mL. **B:** Dependence of the fluorescence intensity at 345 nm (△) and the CD signal at 220 nm (●) on pH. The fluorescence intensity at 356 nm (□) of a solution of *N*-acetyltryptophanamide was measured under identical conditions. CD measurements were made in a 0.1-cm-pathlength cell at a protein concentration of 100 μg/mL. The composition of all buffers is described in Materials and methods.

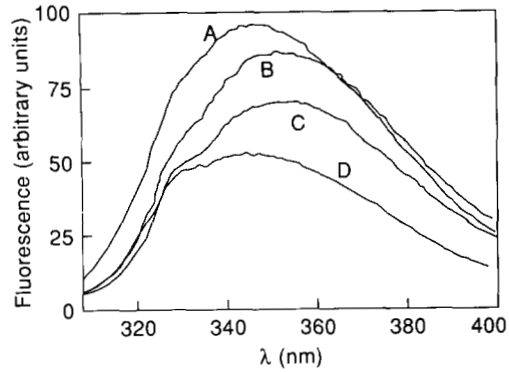

Fig. 3. Effect of denaturation of recombinant mIL-6 by GdnHCl on the fluorescence emission spectrum. Spectra were recorded at 25 °C using a 295-nm excitation wavelength and 2.5-nm and 5-nm excitation and emission slits, respectively. Protein samples contained 44 μg/mL mIL-6. Spectra refer to mIL-6 in the following buffer systems: 10 mM HEPES, pH 7.4 (A); 10 mM HEPES, 6 M GdnHCl, pH 7.4 (B); 10 mM sodium acetate, 6 M GdnHCl, pH 4.0 (C); and 10 mM sodium acetate, pH 4.0 (D). mIL-6 was incubated for 1 h in the appropriate buffer system prior to recording of the spectra.

Denaturation of mIL-6 with 6 M GdnHCl at either pH 4.0 or pH 7.4 resulted in a significant red shift in the emission maximum to 353 nm (Fig. 3). Interestingly, under denaturing conditions the fluorescence of mIL-6 was still quenched (20%) at pH 4.0 (spectra C), relative to pH 7.4 (spectra B).

Because only one of the two tryptophan residues in mIL-6 is conserved (Trp-160) in the human protein (Trp-36 is replaced in hIL-6 with a glutamic acid residue), the latter promised to provide a further insight into the nature of the fluorescent quenching in mIL-6. As expected for a protein with one rather than two tryptophan residues, the overall fluorescence quantum yield of hIL-6 was approximately 50% of that observed for mIL-6 (data not shown). However, in contrast to that observed for mIL-6, only a small overall decrease in emission intensity (~12%) was observed for hIL-6 upon decreasing the pH from 7.4 to 4.0; and in the presence of 6 M GdnHCl the difference in quantum yield was even less (5%).

Circular dichroism studies on mIL-6

The stability of mIL-6 as a function of pH was also assessed by CD spectroscopy in the near and far UV. The "predicted" secondary structural content of mIL-6 based on its far-UV CD spectrum (52% α-helix, 10% β-sheet, 19% random coil, and 19% β-turn) (Zhang et al., 1992) was stable over the pH range 2.5–10.0 (Fig. 2B). Possible pH-induced conformational transitions in mIL-6 were further analyzed using near-UV CD (Fig. 4). Although the near-UV spectra were similar at pH 4.0 and 7.4 (spectra A and B, respectively), the magnitude of the CD band was more intense at pH 4.0. The near-UV CD spectra at both pH values were characterized by major minima at 282 nm, with shoulders being observed at 305, 287, 269, and 263 nm. The major CD transition with a minimum at 282 nm is presumably due to contributions of tyrosine residues (Strickland, 1974). There is no readily assignable tryptophan CD fine structure in the region 290–305 nm that could be easily distinguished from the cystinyl chromophore background. The broad CD band extending above 310 nm may be due to the two disulfide bonds in mIL-6 (Strickland, 1974). A maximum of small positive ellipticity is observed at 255 nm. The positive CD band at 255 nm, also observed for hIL-6 (Krüttgen et al.,

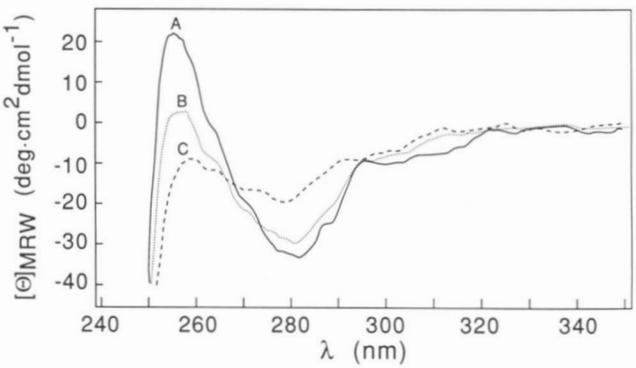

Fig. 4. Effect of pH on near-UV CD spectra of recombinant mIL-6. mIL-6 in 10 mM sodium acetate, pH 4.0 (A); 10 mM Tris-HCl, pH 7.4 (B); and 10 mM Tris-HCl, 6 M GdnHCl, pH 7.4 (C). Spectra were recorded in a 1-cm-pathlength cell at a protein concentration of 1 mg/mL. Results are expressed in terms of mean residue ellipticity, $[\theta]_{MRW}$.

1990) and neurophysin (Breslow, 1970), is also probably due to the cystine chromophores.

Urea-gradient gel electrophoresis

The single folding–unfolding transition observed at both pH 4.0 and 10.2 reveals that mIL-6 is a single conformer under these conditions (Fig. 5). The transitions were cooperative indicating that mIL-6 was not denatured and that it has a compact structure at both pH 4.0 and pH 10.2. The unfolding process was readily reversible at all pH values studied as evidenced by identical transitions when mIL-6 was applied to the gel either directly in buffer or in buffer containing 8 M urea. A continuous band of protein observed throughout the transition region at pH 4.0 indicated that the kinetics of the folding–unfolding process are rapid relative to the electrophoretic separation process (Creighton, 1980). However, at pH 10.2 a discontinuity was observed throughout the transition region, indicating that the rates of folding and unfolding were slow relative to the electrophoretic migration rates. Interestingly, at the intermediate pH value of 8.0 an essentially flat transition region was observed.

It is unlikely that mIL-6 is folded at pH 4.0 and pH 10.0 but unfolded at pH 8.0, particularly in light of the above fluorescence and CD data and the known biological activity of mIL-6 at pH 7.4 (Zhang et al., 1992). Because the relative rates of migration of the native and denatured states of proteins using urea-gradient gel electrophoresis are dependent on both the radii and the net charge of the folded and unfolded states (Hollecker & Creighton, 1982), it must be assumed that at pH 8.0 the relative rates of migration of the folded and unfolded forms of recombinant mIL-6 are being influenced by factors other than the increased radius of the unfolded form. At pH 8.0 mIL-6 has a net charge of only −2.12 (determined as described by Skoog & Wichman [1986]), compared to +16.39 and −11.32 at pH 4.0 and 10.0, respectively. Therefore, a

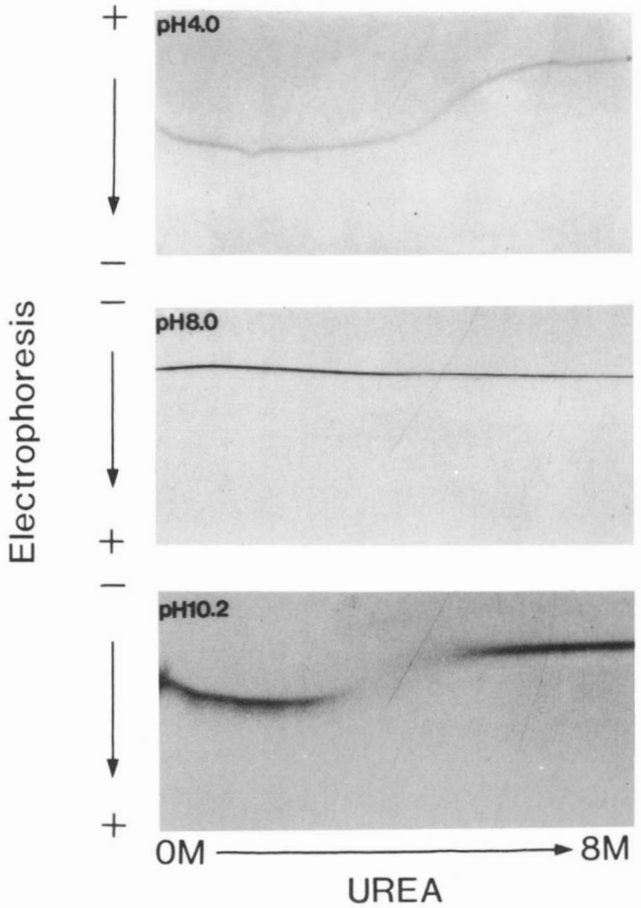

Fig. 5. Urea-gradient gel electrophoresis of mIL-6. Purified mIL-6 (100 μg/mL) was applied across the slab gel containing a transverse gradient of 0–8 M urea. Electrophoresis was performed at pH 4.0, 8.0, and 10.2 as described in the Materials and methods. Protein was visualized by Coomassie blue staining.

small differential in exposure of charged groups between the folded and unfolded states would be expected to have a large effect on the relative rates of migration of the native and denatured states of the molecule. This could then explain the seemingly anomalous migration pattern under these conditions.

Fluorescence characteristics of a synthetic peptide corresponding to the putative helix A of mIL-6

As mentioned above, the pH-dependent quenching of mIL-6 fluorescence was characterized by a midpoint pH value of 6.9 (Fig. 2), a value consistent with the titration of a histidine residue. Of the two tryptophan residues in mIL-6, only one (Trp-36) has a histidine residue (His-33) in close proximity in the polypeptide chain. To test whether the imidazole side chain of His-33 could quench the fluorescence of the indole ring of Trp-36, the peptide Val-Gly-Gly-Leu-Ile-Thr-His-Val-Leu-Trp-Glu-Ile-Val-Glu-Met-Arg-Lys (peptide H1), which corresponds to res-

idues 27–43 in helix A in the postulated 4-α-helical bundle structure of mIL-6 (Parry et al., 1991), was synthesized.

Figure 6A reveals a 28% decrease in fluorescence intensity of peptide H1 upon decreasing the pH from 7.4 to 4.0 (spectra C, D). In the presence of 6 M GdnHCl this decrease was slightly more pronounced (30%) (spectra A, B). The maximum was 352 nm in the presence and absence of GdnHCl, indicating that Trp-36 was totally exposed to solvent under both conditions. This is consistent with the far-UV CD spectrum of peptide H1, which had little defined secondary structure in aqueous media at pH 4.0 as judged by far-UV CD (Fig. 7). The CD spectrum of peptide H1 in 10 mM sodium acetate, pH 4.0 (spectrum D) is characterized by a major minimum at 200 nm, which is typical of a disordered, predominantly random coil conformation (Yang et al., 1986). Presumably, the increased fluorescence emission of peptide H1 upon the addition of GdnHCl indicates that interactions that quench Trp-36 in the random coil conformation occur more efficiently in the absence of denaturant. The CD spectra were also measured in aqueous TFE and aqueous SDS. TFE appears to stabilize the secondary structure for which a peptide has a propensity to form (Zhong & Johnson, 1992). SDS has also been shown to induce secondary structure formation in some peptides (Bansal et al., 1990; Zhong & Johnson, 1992); in the case of proteins, the situation is much more complex (Mattice et al., 1976). In aqueous 30% TFE and 50 mM aqueous SDS, the far-UV CD spectra in both solutions revealed minima at 220 nm and 208 nm, which are characteristic of peptides or proteins possessing a high percentage of helical content (Fig. 7, spectra A and B). In 50 mM SDS the spectra were identical at pH 4.0 and 7.4. In TFE however, helix formation was favored at pH 4.0 (Fig. 7, spectrum B) relative to pH 7.4 (Fig. 7, spectrum C). The α-helical content of peptide H1 in 50 mM SDS at pH 4.0, 30% TFE at pH 4.0, and 30% TFE at pH 7.4 were estimated (see Materials and methods) to be 58, 58, and 26%, respectively. The pH dependence of peptide H1 fluorescence spectra in buffers containing 50 mM SDS is shown in Figure 6B. Upon going from pH 9.4 to pH 4.0 the fluorescence intensity was decreased by 62%. Similar quenching was also observed in the presence of 30% TFE, a 53% decrease occurring upon going from pH 7.4 to pH 4.0 (data not shown). The fluorescence intensity of *N*-acetyltryptophanamide in the presence of SDS did not change over the same pH range (data not shown). The quenching of the peptide fluorescence was accompanied by a small blue shift of the fluorescence emission maximum, from 352 nm at pH 9.4 (Fig. 6B, spectrum A) to 344 nm at pH 4.1 (Fig. 6B, spectrum I). Interestingly, this finding is similar to that for mIL-6 and reflects the transfer of Trp-36 to a less polar environment.

The possible involvement of His-33 in the pH-dependent fluorescence quenching of Trp-36 in mIL-6 and its role

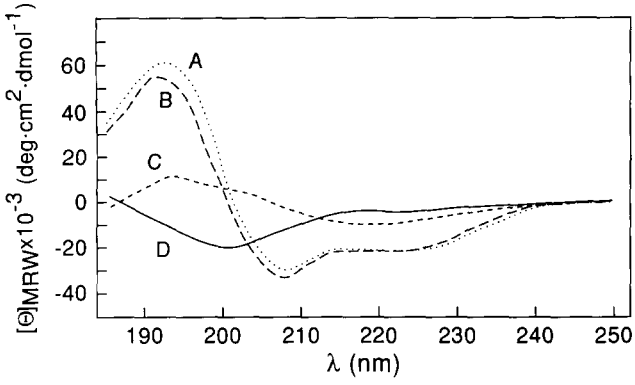

Fig. 7. Far-UV CD spectra of peptide H1 measured under various conditions. All spectra were obtained at 25 °C using a 0.1-cm-pathlength cell at a protein concentration of 141 μg/mL. The spectra were recorded under the following buffer conditions: 10 mM sodium acetate, 50 mM SDS, pH 4.0 (A); 10 mM sodium acetate, 30% TFE, pH 4.0 (B); 10 mM Tris-HCl, 30% TFE, pH 7.4 (C); and 10 mM sodium acetate, pH 4.0 (D).

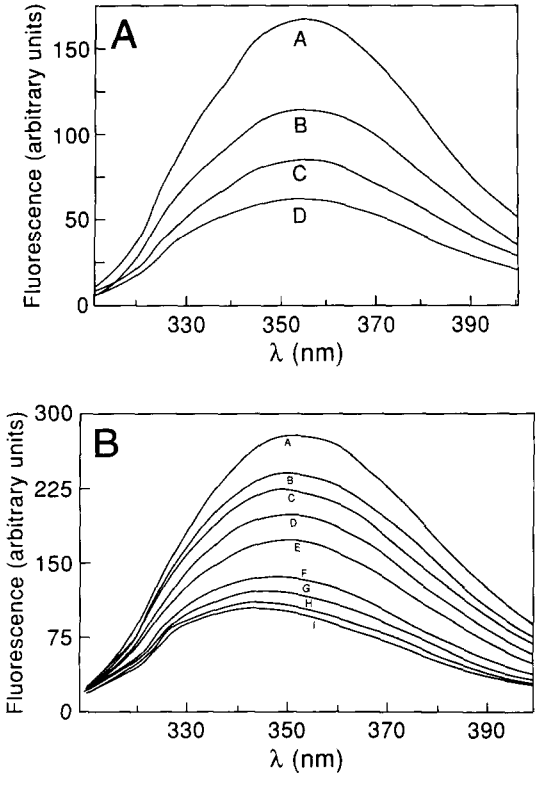

Fig. 6. Fluorescence spectra of synthetic peptide H1 (Val-27–Lys-43 of mIL-6 sequence). **A:** Effect of 6 M GdnHCl and pH. Spectra were recorded in the following buffer systems: 10 mM HEPES, 6 M GdnHCl, pH 7.4 (A); 10 mM sodium acetate, 6 M GdnHCl, pH 4.0 (B); 10 mM HEPES, pH 7.4 (C); and 10 mM sodium acetate, pH 4.0 (D). **B:** Effect of pH in buffers containing 50 mM SDS. Peptide H1 was incubated in buffers of the following pH containing 50 mM SDS: pH 9.4 (A), pH 8.4 (B), pH 7.9 (C), pH 7.3 (D), pH 6.8 (E), pH 6.1 (F), pH 5.6 (G), pH 5.1 (H), and pH 4.1 (I). The buffer compositions are described in Materials and methods. All spectra were recorded at 25 °C using an excitation wavelength of 295 nm and a peptide concentration of 7.3 μg/mL.

in influencing the conformational properties of peptide H1 was further probed using a synthetic peptide (peptide H1a), which is identical to peptide H1 except that His-33 is replaced with an alanine residue. The effect of pH on the fluorescence spectra of peptide H1a in the presence and absence of 6 M GdnHCl is summarized in Figure 8A. This His-33/Ala-33 substitution resulted in a similar, but decreased, extent of pH-dependent quenching, 13% in the absence (Fig. 8A, spectra C, D) and 14% in the presence of GdnHCl (Fig. 8A, spectra A, B). This compares with the 28 and 30% decreases in quantum yield observed for peptide H1 under the same conditions (Fig. 6A).

The residual pH-dependent quenching obtained for peptide H1a suggests that other amino acids in addition to His-33 are involved in the quenching of Trp-36 fluorescence. The pH dependence of the observed fluorescence intensity at 352 nm for both peptide H1 and H1a (Fig. 9A) supports this conclusion. For peptide H1a the fluorescence quenching curve has a midpoint of pH 4.5. For peptide H1 however, quenching occurs over a broader pH range, extending from 8.0 to 3.0 (midpoint pH 7.0).

Replacement of His-33 with an alanine residue had a significant effect on the conformational properties of the peptide H1. Whereas peptide H1 possesses a predominantly random coil conformation in the absence of sec-

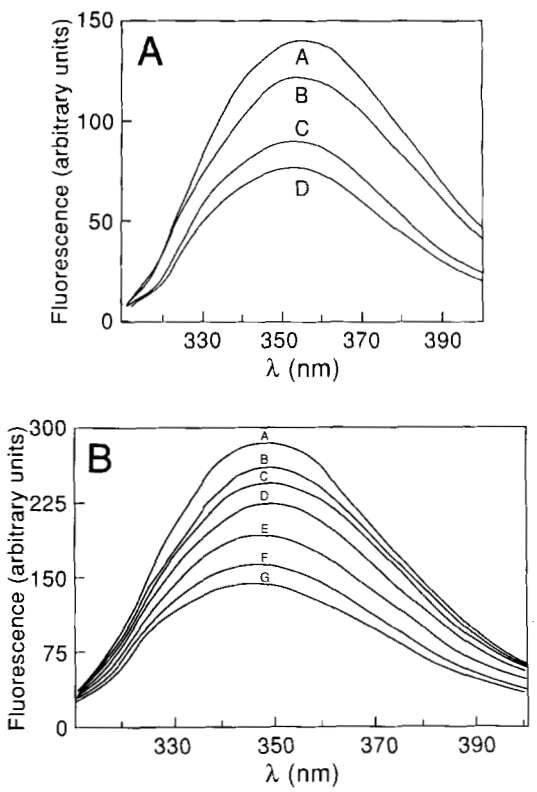

Fig. 8. Dependence of the fluorescence spectra of peptide H1a (peptide H1 with a His-33/Ala-33 substitution) on pH. **A:** Effect of denaturant and pH. The fluorescence spectra of peptide H1a were recorded in the following buffer systems: 10 mM HEPES, 6 M GdnHCl, pH 7.4 (A); 10 mM sodium acetate, 6 M GdnHCl, pH 4.0 (B); 10 mM HEPES, pH 7.4 (C); and 10 mM sodium acetate, pH 4.0 (D). **B:** Effect of pH on the fluorescence emission spectrum of peptide H1a when incubated in the presence of the helix-promoting agent SDS. The peptide was incubated in buffers containing 50 mM SDS with the following pH values: pH 9.4 (A), pH 8.4 (B), pH 7.3 (C), pH 6.8 (D), pH 6.1 (E), pH 5.1 (F), and pH 4.1 (G). The buffer compositions are described in Materials and methods. Spectra were recorded at 25 °C using an excitation wavelength of 295 nm and a peptide concentration of 7.3 μg/mL.

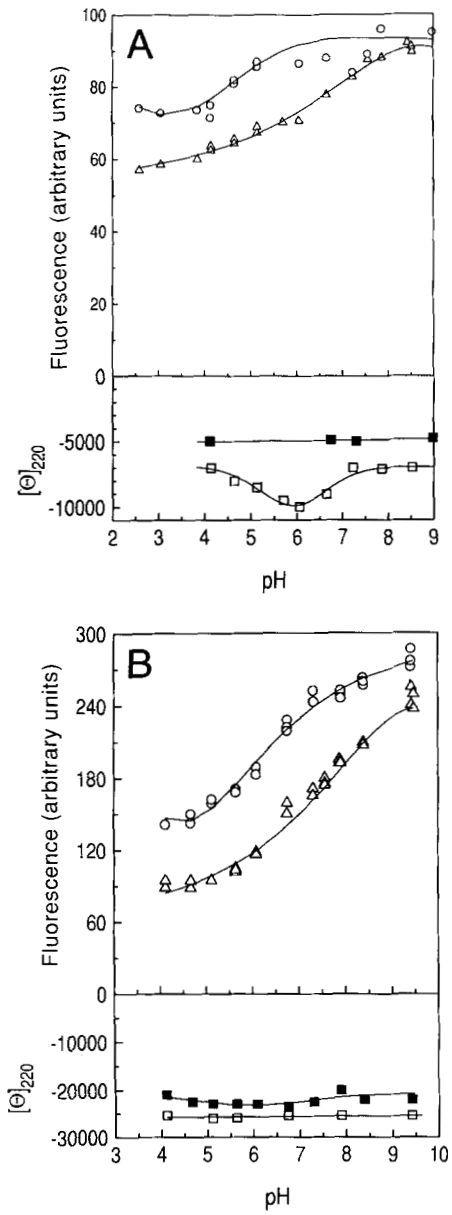

Fig. 9. Influence of pH on the fluorescence and the CD signals of synthetic peptides H1 and H1a. All measurements were performed at 25 °C using a peptide concentration of 7.3 μg/mL. Measurements were made in the absence (**A**) and presence (**B**) of the helix-promoting agent SDS (50 mM). Fluorescence signal (at 352 nm) of peptide H1 (△) and peptide H1a (○); CD signal (at 220 nm) ($[\theta]_{220}$) of peptide H1 (■) and peptide H1a (□).

ondary structure-inducing solvents (Fig. 7, spectrum D), peptide H1a had a far-UV CD spectrum indicative of the presence of a small proportion of α-helix (Fig. 10, spectrum A). At a concentration of 7.3 μg/mL, the same concentration as that used in the fluorescence studies, the helical content of the peptide was highest at pH 6.0. This is illustrated in Figure 9, the relative propensity of both peptide H1 and H1a to form α-helix being monitored by the ellipticity at 220 nm ($[\theta]_{220}$). When adopting a helical conformation, peptide H1 would be expected to be amphiphilic with distinct hydrophobic and hydrophilic faces being predicted from helical wheel analysis (Fig. 11). To test the possibility that peptide H1a was adopting a partially helical conformation as a result of self association of the peptide along its hydrophobic face, the concentration dependence of the process was investigated. Helix formation was not dependent on the concentration of peptide, essentially identical spectra being observed over the concentration range 0.7–70 μg/mL in 10 mM acetate, pH 5.0 (data not shown).

The propensity of peptide H1a to form an α-helix was further enhanced in the presence of 50 mM SDS (Fig. 10, spectrum B), α-helical contents of 29% and 76% being calculated in the absence and presence of SDS, respectively. The pH dependence of the fluorescence spectra of peptide H1a in the presence of 50 mM SDS is illustrated in Figure 8B. Upon decreasing the pH from 9.4 to 4.1, the fluorescence emission intensity of peptide H1a was decreased 45% in comparison to the 63% observed for peptide H1 (Fig. 9B). The wavelength of maximum fluorescence emission for peptide H1a was blue shifted from 352 nm to 348 nm over the same pH range. There was no significant change in the secondary structure of peptide H1a in the presence of SDS from pH 4 to 9.4 as judged by the constancy of $[\theta]_{220}$ (Fig. 9B). Thus, although His-33 contributes to the quenching of Trp-36 fluorescence in the presence of helix-inducing SDS, other amino acids in the peptide are also involved.

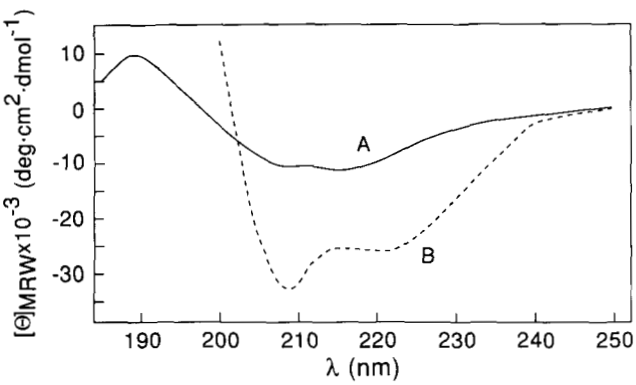

Fig. 10. Far-UV CD spectra of synthetic peptide H1a. Both spectra were obtained at 25 °C using a 1-cm-pathlength cell and a protein concentration of 7.3 μg/mL: 10 mM sodium acetate, pH 5.0 (A); and 10 mM sodium acetate, 50 mM SDS, pH 5.0 (B).

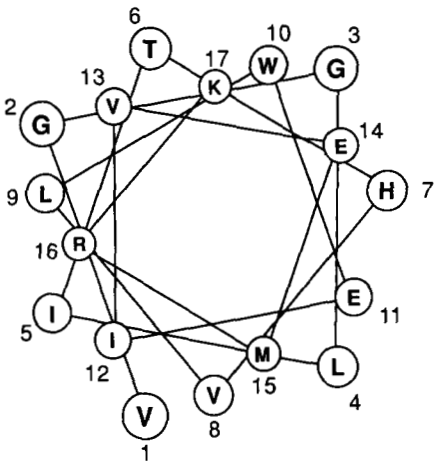

Fig. 11. Helical-wheel analysis of peptide H1. Residues 1–17 correspond to residues Val-27–Lys-43 of the murine IL-6 amino acid sequence.

Discussion

In this study, we found that the intrinsic tryptophan fluorescence of mIL-6 was quenched 40% upon decreasing the pH from 8.5 to 4.0; the midpoint of the transition being pH 6.9. The quenching of tryptophan fluorescence was not accompanied by a red shift in the emission maximum suggesting that mIL-6 is not unfolding over this pH range. This finding was corroborated by far-UV CD measurements, which revealed no appreciable change in the secondary structure of the molecule over this pH range. Weight average molecular weights of 19,800 and 22,500 were calculated by sedimentation equilibrium centrifugation at pH 4.0 and 7.4, respectively. There was no sign of concentration-dependent self-association from 0.1 to 0.3 mg/mL mIL-6. Because the fluorescence experiments were performed at a protein concentration of 0.03 mg/mL, displacement of a monomer–polymer equilibrium by pH cannot be assumed to be responsible for the quenching of fluorescence.

On the basis of the drastic decrease in the fluorescence emission intensity over the pH range 8.5 to 4.0, a change in the environment of tryptophan residues and, consequently, the near-UV CD spectrum would be expected. Accordingly, differences in the near-UV CD spectra of mIL-6 at pH 4.0 and pH 7.4 were also observed. These changes were manifested as more intense CD signals at pH 4.0, relative to pH 7.4, the overall shape of the spectra being similar at both pH values. Whether the experimental observations reflected only changes in the environment of the tryptophan residues (rather than other aromatic residues, for example, tyrosine residues) is not clear because no obvious tryptophan transition was observed in the region 290–300 nm. The observed fluorescence emission maximum of the molecule (345–349 nm depending on pH) could reflect that both tryptophan side chains in mIL-6 are partially exposed to solvent (Lakowicz, 1983).

Such exposure could then lead to a lack of constraint of the tryptophan residues in the tertiary structure. The aromatic amino acids tryptophan, tyrosine, and phenylalanine only exhibit an appreciable CD signal when they are present in asymmetric environments (Strickland, 1974). The accessibility of both tryptophan side chains to solvent is also consistent with chemical modification studies in which both tryptophan residues of mIL-6 were readily modified under mild nondenaturing conditions (unpubl. data).

Alternatively, the lack of a CD signal at 295 nm, may be due to the fortuitous cancelling of both positive and negative ellipticities of the indole rings for Trp-36 and Trp-160. To shed light on this possibility we compared the CD spectra of m- and hIL-6. Only Trp-160 of mIL-6 is conserved in the primary amino acid sequence of hIL-6. The near-UV CD spectrum of hIL-6 is similar to that of mIL-6, being dominated by a minimum at 277 nm and possessing a small positive maximum at 253 nm (Krüttgen et al., 1990). No distinct tryptophan transition at 295 nm was observed for hIL-6, indicating that Trp-160 is most likely to be in an unconstrained environment. Further evidence for Trp-160 in hIL-6 being solvent-exposed is provided by chemical modification and NMR studies reported by Nishimura and coworkers (1990).

Our finding that the tryptophan fluorescence of mIL-6, in the presence of 6 M GdnHCl, was still quenched 20% at pH 4.0 relative to pH 7.4 suggests that amino acids vicinal to tryptophan residues are partially responsible for this phenomenon. This notion was supported by the demonstration of significant fluorescence quenching (~30%), in the presence or absence of GdnHCl, of Trp-36 in the synthetic peptide H1, which corresponds to residues Val-27–Lys-43 in the putative helix A of mIL-6.

In the 4-α-helical bundle model of mIL-6 proposed by Parry and coworkers (1991) His-33 and Trp-36 lie in the i and $i+3$ position on the surface of helix A, thereby allowing ready interaction between the side chains of these two amino acids in the native conformation. Such an interaction is supported by NMR studies, which show interactions between a histidine and tryptophan residue in mIL-6 (in prep.). The interatomic distance observed was consistent with an i and $i+3$ arrangement in an α-helix. Although peptide H1 had little tendency to form an α-helix in aqueous buffer systems, aqueous TFE or SDS induced a predominantly α-helical conformation (58% as assessed from far-UV CD). In aqueous SDS the fluorescence of Trp-36 in peptide H1 is markedly more pH dependent, the fluorescence being quenched 62.5% on going from pH 9.4 to pH 4.0, compared to 28% in the absence of SDS. This is consistent with residues responsible for quenching being brought into closer proximity to Trp-36 upon formation of α-helical secondary structure. Because mIL-6 fluorescence is quenched more in the native state, relative to the denatured state, this is consistent with residues in this putative α-helical secondary structural element being directly involved in the quenching of Trp-36 in the native molecule.

Amino acids in peptide H1 that would be predicted to quench, in a pH-dependent manner, include the α-amino group and Lys-43 His-33, Glu-37, and Glu-40. The protonated form of histidine (Shinitzky & Goldman, 1967; Loewenthal et al., 1991) and unionized carboxylic acid groups (White, 1959; Cowgill, 1963) have been demonstrated to be efficient quenchers of tryptophan fluorescence. Both protonated and deprotonated amino groups (White, 1959; Cowgill, 1963; Edelhoch et al., 1967; Shinitzky & Goldman, 1967) have the ability to quench tryptophan fluorescence, the distance of the amine group from the indole in the excited state dictating which form is the more efficient quencher (Edelhoch et al., 1967). In the case of peptide H1, His-33 was shown to be partially responsible for this quenching because replacement of His-33 with an alanine residue (in peptide H1a) reduced quenching from 30% to 15% in the random coil conformation and from 63 to 45% in the presence of SDS, which seems to induce α-helix in this system. Due to both their proximity and the observed midpoint describing the pH-dependent fluorescence, Glu-37 and Glu-40 are the most likely amino acids to be responsible for the remainder of the fluorescence quenching. However, it should be stressed that the high charge density of bound SDS may influence the pK_a of quenching amino acids. Consequently, care must be taken in terms of interpreting the data to indicate that an amino acid of a particular pK_a value is involved. In the absence of the helix-promoting SDS, the midpoint of the quenching transition shifted from 7.0 to 4.5 upon removal of His-33.

In this study we have demonstrated that the fluorescence of mIL-6 is quenched upon decreasing the pH. This acid quenching does not appear to be due to a global unfolding of the protein but rather to local changes in the vicinity of one or both of the tryptophan residues of mIL-6. Peptide H1 (Val-27–Lys-43), corresponding to the putative helix A of mIL-6 (Parry et al., 1991) was shown to possess many of the pH-dependent fluorescence characteristics of mIL-6. As acid quenching of the fluorescence of synthetic peptide H1 was more pronounced in the presence of helix-promoting solvents, we postulate that residues brought into close proximity to Trp-36 in the putative helix A of mIL-6 are contributing significantly to the acid quenching of the native protein. This region of mIL-6 has been proposed to be important in receptor binding using a number of criteria. For instance, whereas hIL-6, N-terminally truncated lacking the first 27 residues, is fully active, the successive removal of residues 28–33 causes a drastic reduction in biological activity (Brakenhoff et al., 1989). Neutralizing monoclonal antibodies have also been demonstrated to bind to the region incorporating part of the putative helix A of hIL-6 (Brakenhoff et al., 1990). By analogy to other receptor systems, the corresponding region of GM-CSF was shown

to be principally involved in binding to the β-subunit of the GM-CSF receptor (Shanafelt et al., 1991). It was noted by these authors that, when aligned with other cytokines, an acidic residue (Glu-37 in mIL-6) was conserved in all cytokines belonging to this four-α-helical bundle family, thereby implying the importance of this acidic residue in receptor binding.

If the unusual fluorescence quenching of mIL-6 can be attributed to the interaction of Trp-36 with particular residues in the amino-terminal helix this phenomenon will provide a convenient probe for monitoring the conformational state of this region of mIL-6. Site-directed mutagenesis studies designed to investigate the influence of His-33, Trp-36, Glu-37, and Glu-40 on receptor binding, bioactivity, and the physicochemical properties of mIL-6 are currently underway.

Materials and methods

Materials

Recombinant mIL-6 was purified from *E. coli*, strain JM101, which carries the mIL-6 gene on the *lac* operon-inducible plasmid pUC9 (Simpson et al., 1988b), as previously described (Zhang et al., 1992). Recombinant hIL-6 was purified in a similar manner.

GdnHCl (8 M stock solution) was purchased from Pierce (Rockford, Illinois). Acrylamide, bis-acrylamide, urea, and SDS were from Bio-Rad (Richmond, California). *N*-acetyltryptophanamide was obtained from Sigma (St. Louis, Missouri). All buffers were prepared with deionized water purified by a tandem Milli-RO and Milli-Q system (Millipore, Bedford, Massachusetts).

Methods

Solid-phase peptide synthesis

Peptide H1 (VGGLITHVLWEIVEMRK) corresponding to amino acid residues Val-27–Lys-43 of the mIL-6 sequence (Simpson et al., 1988a) and peptide H1a (VGGLITAVLWEIVEMRK), containing a His-33/Ala-33 substitution, were synthesized using solid-phase peptide chemistry incorporating 2-(1H-benzotriazol-1-yl)-1,1,3,3-tetramethyluronium tetrafluoroborate 1-hydroxybenzotriazole coupling chemistry and tert-butyloxycarbonyl-based chemistry (Reid & Simpson, 1992).

Fluorescence spectroscopy

Fluorescence measurements of the intrinsic protein fluorescence of mIL-6 were performed on a Perkin Elmer LS-5 Luminescence Spectrometer. For pH-dependent fluorescence measurements, mIL-6 (1 mg/mL in H_2O) was diluted to a concentration of 30 μg/mL in the following buffer systems: 10 mM sodium acetate (pH 4.0, 4.5, 5.0, 5.5), 10 mM MES (pH 5.9, 6.5), 10 mM HEPES (pH 7.0, 7.5), and 10 mM Tris-HCl (pH 8.0, 8.5). Solutions were incubated for 1 h prior to the recording of fluorescence spectra using a 295-nm excitation wavelength. Fluorescence spectra of *N*-acetyltryptophanamide (5.48×10^{-6} M) were recorded under identical conditions, the concentration being calculated using a molar extinction coefficient of 5,600 M^{-1} at 280 nm (Brems et al., 1985).

For denaturant-induced unfolding experiments employing fluorescence spectroscopy, a stock solution of mIL-6 (1 mg/mL) was diluted to 40 μg/mL in either 10 mM sodium acetate, pH 4.0 or 10 mM Tris-HCl buffer, pH 7.4, containing the appropriate concentrations of GdnHCl.

Circular dichroism spectroscopy

CD spectra were recorded using an Aviv Model 62DS CD spectrometer at 25 °C. Far-UV CD spectra were performed at protein concentrations of 50–200 μg/mL (as indicated in the text) using a 0.1-cm-pathlength cell, while near-UV CD spectra were obtained at a protein concentration of 1 mg/mL using a 1-cm-pathlength cell. Buffer blanks were subtracted from all spectra. Reported spectra are expressed in terms of mean residue ellipticities $[\theta]_{MRW}$, which were calculated using a mean residue weight of 115.3. For pH-dependence experiments, a stock solution of mIL-6 (1 mg/mL) was diluted to 50 μg/mL in the following buffers: 10 mM sodium phosphate (pH 2.51, 3.05, 4.3, 7.7) and 10 mM Tris-HCl (pH 7.2, 10.0). Solutions were incubated for 1 h at 25 °C, prior to the recording of far-UV CD spectra.

The fractional percent helix for the peptides was estimated on the basis of the value of $[\theta]_{222}$, as described by Chakrabarty et al. (1991). The theoretical ellipticity at 222 nm for a peptide possessing 100% helical character was taken to be equal to $-40{,}000\ (1 - 2.5/n)$, where n is the number of amino acids in the peptide. The calculated value for peptide H1 is 34,117 deg cm^2 $dmol^{-1}$. A value of 0 deg cm^2 $dmol^{-1}$ was used as the value of $[\theta]_{222}$ representing 0% helix.

Analytical ultracentrifugation

Sedimentation experiments were carried out at 20 °C in a Beckman Model E ultracentrifuge fitted with an electronic speed control and an RTIC temperature control. Sedimentation velocity experiments were performed at 56,000 rpm in a synthetic boundary cell and the boundary monitored using a Schlieren optical system. The symmetrical nature of the boundaries obtained for mIL-6 allowed S (the weight average sedimentation coefficient) to be determined by the rate of migration of the Schlieren peak. Sedimentation equilibrium experiments were carried out at 44,000 rpm for 22 h, the equilibrium solute distribution being recorded as Rayleigh interferograms.

Urea-gradient electrophoresis

Urea-induced unfolding of mIL-6 was monitored by urea gradient gel electrophoresis, essentially as described

by Goldenberg (1990). Briefly, slab gels (6 cm × 8.8 cm × 0.1 cm) were prepared containing a transverse gradient of 0–8 M urea with an inverse gradient of 15–11% acrylamide in order to compensate for the electrophoretic effects of the urea. Unfolding of mIL-6 was monitored using the following buffer conditions: (1) 50 mM acetate-Tris, pH 4.0, (2) 50 mM Tris-acetate, pH 8.0, and (3) 20 mM CAPS-ammonia, pH 10.2. Electrophoresis of protein (~100 μg/mL) was performed in a Bio-Rad Mini-Protean® apparatus at 25 °C for 3 h at 6, 12, or 5 mA constant current for the pH 4.0, pH 8.0, and pH 10.2 buffers, respectively. Pre-electrophoresis was performed for 1 h prior to electrophoresis in all cases. Protein was visualized by staining the gel with Coomassie brilliant blue R250 as previously described (Zhang et al., 1992).

Acknowledgments

We are indebted to Robert L. Moritz for purifying recombinant mIL-6 and to Gavin E. Reid for synthesizing the peptides used in this study. This work was supported by grant number 920528 from the National Health and Medical Research Council of Australia.

References

Bansal, A., Stradley, S.J., & Gierasch, L.M. (1990). Conformational studies of peptides corresponding to the LDL receptor cytoplasmic tail and transmembrane domain. In *Current Research in Protein Chemistry II* (Villafranca, J.J., Ed.), pp. 331–338. Academic Press, San Diego.

Brakenhoff, J.P.J., Hart, M., & Aarden, L. (1989). Analysis of human IL-6 mutants expressed in *Escherichia coli*. Biological activities are not affected by deletion of amino acids 1–28. *J. Immunol. 143*, 1175–1182.

Brakenhoff, J.P.J., Hart, M., de Groot, E.R., Di Padova, F., & Aarden, L.A. (1990). Structure–function analysis of human IL-6: Epitope mapping of neutralizing monoclonal antibodies with amino- and carboxyl-terminal deletion mutants. *J. Immunol. 145*, 561–568.

Brems, D.N., Plaisted, S.M., Havel, H.A., Kauffman, E.W., Stodola, J.D., Eaton, L.C., & White, R.D. (1985). Equilibrium denaturation of pituitary- and recombinant-derived bovine growth hormone. *Biochemistry 24*, 7662–7668.

Breslow, E. (1970). Optical activity of bovine neurophysins and their peptide complexes in the near ultraviolet. *Proc. Natl. Acad. Sci. USA 67*, 493–500.

Chakrabarty, A., Schellman, J.A., & Baldwin, R.L. (1991). Large differences in the helix propensities of alanine and glycine. *Nature 351*, 586–588.

Cohn, E.J. & Edsall, J.T. (1943). *Proteins, Amino Acids and Peptides*. Van Nostrand-Reinhold, Princeton, New Jersey.

Cowgill, R.W. (1963). Fluorescence and the structure of proteins I. Effects of substituents on the fluorescence of indole and phenol compounds. *Arch. Biochem. Biophys. 100*, 36–44.

Creighton, T.E. (1980). Kinetic study of protein unfolding and refolding using urea gradient electrophoresis. *J. Mol. Biol. 137*, 61–80.

Edelhoch, H., Brand, L., & Wilchek, M. (1967). Fluorescence studies with tryptophanyl peptides. *Biochemistry 6*, 547–559.

Goldenberg, D.P. (1990). Analysis of protein conformation by gel electrophoresis. In *Protein Structure: A Practical Approach* (Creighton, T.E., Ed.), pp. 225–250. IRL Press Ltd., Oxford, UK.

Gordon, M.S. & Hoffman, R. (1992). Growth factors affecting human thrombocytopoiesis: Potential agents for the treatment of thrombocytopenia. *Blood 80*, 302–307.

Hirano, T., Akira, S., Taga, T., & Kishimoto, T. (1990). Biological and clinical aspects of interleukin-6. *Immunol. Today 11*, 443–449.

Hollecker, M. & Creighton, T.E. (1982). Effect on protein stability of reversing the charge on amino groups. *Biochim. Biophys. Acta 701*, 395-404.

Kishimoto, T. (1989). The biology of interleukin-6. *Blood 74*, 1–10.

Klein, B. & Bataille, R. (1991). Recent advances in the biology of IL-6 in multiple myeloma. *Cancer J. 4*, 81–82.

Krüttgen, A., Rose-John, S., Moller, C., Wroblowski, B., Wollmer, A., Mullberg, J., Hirano, T., Kishimoto, T., & Heinrich, P.C. (1990). Structure–function analysis of human interleukin-6. Evidence for the involvement of the carboxy-terminus in function. *FEBS Lett. 262*, 323–326.

Lakowicz, J.R. (1983). *Principles of Fluorescence Spectroscopy*. Plenum Press, New York.

Loewenthal, R., Sancho, J., & Fersht, A.R. (1991). Fluorescence spectrum of barnase: Contribution of three tryptophan residues and a histidine-related pH dependence. *Biochemistry 30*, 6775–6779.

Mattice, W.L., Riser, J.M., & Clark, D.S. (1976). Conformational properties of the complexes formed by proteins and sodium dodecyl sulfate. *Biochemistry 15*, 4264–4272.

Nishimura, C., Hanzawa, H., Itoh, S., Yasukawa, K., Shimada, I., Kishimoto, T., & Arata, Y. (1990). Proton nuclear magnetic resonance study of human interleukin-6: Chemical modifications and partial spectral assignments for the aromatic residues. *Biochim. Biophys. Acta 1041*, 243–249.

Parry, D.A.D., Minasian, E., & Leach, S.J. (1991). Cytokine conformations: Predictive studies. *J. Mol. Recog. 4*, 63–75.

Reid, G.E. & Simpson, R.J. (1992). Automated solid-phase synthesis: Use of 2-(H-benzotriazol-1-yl)-1,1,3,3-tetramethyluronium tetrafluoborate for coupling of tert-butyloxycarbonyl amino acids. *Anal. Biochem. 200*, 301–309.

Shanafelt, A.B., Miyajima, A., Kitamura, T., & Kastelein, R.A. (1991). The amino-terminal helix of GM-CSF and IL-5 governs high affinity binding to their receptors. *EMBO J. 10*, 4105–4112.

Shinitzky, M. & Goldman, R. (1967). Fluorimetric detection of histidine–tryptophan complexes in peptides and proteins. *Eur. J. Biochem. 3*, 139–144.

Simpson, R.J., Moritz, R.L., Rubira, M.R., & Van Snick, J. (1988a). Murine hybridoma/plasmacytoma growth factor: Complete amino-acid sequence and relation to human interleukin-6. *Eur. J. Biochem. 176*, 187–197.

Simpson, R.J., Moritz, R.L., Van Roost, E., & Van Snick, J. (1988b). Characterization of a recombinant murine interleukin-6: Assignment of disulfide bonds. *Biochem. Biophys. Res. Commun. 157*, 364–372.

Skoog, B. & Wichman, A. (1986). Calculation of the isoelectric points of polypeptides from the amino acid composition. *Trends Anal. Chem. 5*, 82–83.

Strickland, D.H. (1974). Aromatic contributions to circular dichroism spectra of proteins. *CRC Crit. Rev. Biochem. 2*, 113–175.

Van Snick, J. (1990). Interleukin-6: An overview. *Annu. Rev. Immunol. 8*, 253–278.

Van Snick, J., Cayphas, S., Szikora, J.-P., Renauld, J.-C., Van Roost, E., Boon, T., & Simpson, R.J. (1988). cDNA cloning of murine interleukin-HP1: Homology with human interleukin-6. *Eur. J. Immunol. 18*, 193–197.

White, A. (1959). Effect of pH on fluorescence of tyrosine, tryptophan and related compounds. *Biochem. J. 71*, 217–220.

Yang, J.T., Wu, C.-S.C., & Martinez, H.M. (1986). Calculation of protein conformation from circular dichroism. *Methods Enzymol. 130*, 208–269.

Yphantis, D.A. (1964). Equilibrium ultracentrifugation of dilute solutions. *Biochemistry 3*, 297–317.

Zhang, J.G., Moritz, R.L., Reid, G.E., Ward, L.D., & Simpson, R.J. (1992). Purification and characterization of a recombinant murine interleukin-6: Isolation of N- and C-terminally truncated forms. *Eur. J. Biochem. 207*, 903–913.

Zhong, L. & Johnson, W.C., Jr. (1992). Environment affects amino acid preference for secondary structure. *Proc. Natl. Acad. Sci. USA 89*, 4462–4465.